Spin-Orbit-Mediated Manipulation of Heavy-Hole Spin Qubits in Gated Semiconductor Nanodevices

P. Szumniak,[1,2] S. Bednarek,[1] B. Partoens,[2] and F. M. Peeters[2]

[1]*Faculty of Physics and Applied Computer Science, AGH University of Science and Technology, al. Mickiewicza 30, 30-059 Kraków, Poland*

[2]*Departement Fysica, Universiteit Antwerpen, Groenenborgerlaan 171, B-2020 Antwerpen, Belgium*

(Received 10 February 2012; published 4 September 2012)

A novel spintronic nanodevice is proposed that is able to manipulate the single heavy-hole spin state in a coherent manner. It can act as a single quantum logic gate. The heavy-hole spin transformations are realized by transporting the hole around closed loops defined by metal gates deposited on top of the nanodevice. The device exploits Dresselhaus spin-orbit interaction, which translates the spatial motion of the hole into a rotation of the spin. The proposed quantum gate operates on subnanosecond time scales and requires only the application of a weak static voltage which allows for addressing heavy-hole spin qubits individually. Our results are supported by quantum mechanical time-dependent calculations within the four-band Luttinger-Kohn model.

DOI: 10.1103/PhysRevLett.109.107201 PACS numbers: 75.76.+j, 03.67.Lx, 71.70.Ej, 85.75.−d

There is currently great interest in studying spin related phenomena in semiconductors. On the one hand there is novel fundamental physics at the nanoscale and on the other hand one expects applications in terms of spin based quantum information processing [1,2]. Physical realization of quantum computers requires fulfillment of a number of challenging criteria [3]. A fragile quantum state has to be coherent for sufficient long time which usually requires its isolation from the environment. On the other hand it has to be externally manipulated. For these purposes, the electron spin in semiconductor quantum dots was suggested as a promising candidate [4]. There are a number of experiments in which the electron spin is initialized, manipulated, stored, and read out [5–11].

Usually spin-state manipulation requires the application of microwave radiation, radio-frequency electric fields as well as magnetic fields. These methods strongly limits the possibility to address spins qubits individually. The first step towards selective control of individual single electron spins was demonstrated in recent state of the art experiments [12,13]. Electron spin manipulation was realized by means of electric fields which can be generated locally quite easily and indirectly via spin orbit interaction which couples charge and spin degrees of freedom. Electron spin control based on spin orbit effect was also proposed in some theoretical papers [14–18].

Unfortunately, in most semiconductor quantum dots the electron spin is exposed to hyperfine interaction with nuclear spins which are present in the host material. This interaction is then the main source of electron spin decoherence in quantum dots putting a severe restriction on the possibility to realize a highly coherent electron spin qubit [19,20]. There are several appealing ideas how to deal with this type of decoherence in quantum dot systems [21]. Very promising way to eliminate or reduce the contact hyperfine interaction with the nuclear spin lattice is to use the spin state of the valence holes—a missing electron in the valence band—as a carrier of quantum information instead of electrons. Holes are described by the p orbitals that vanish at a nuclear site, which strongly suppresses the Fermi hyperfine contact interaction. Thus one can expect longer coherence times for hole spin states [22,23]. Some experiments seem to confirm this statement reporting long relaxation ($\sim$ms) and coherence ($\sim\mu$s) times [24–27] for hole spins while others reported a very short hole spin dephasing time ($\sim$ns) [28]. Recent theoretical investigations [29,30] and experiments [31] seem to resolve this mismatch of coherence times in different experiments suggesting that the absence of mixing between the heavy-hole (HH) and the light-hole(LH) state is crucial for a long hole spin coherence time. Not only long coherence times but also the possibility to initialize the hole spin state even without a magnetic field [25], and the recent realization of a coherent control of a hole spin state in single and double coupled quantum dots [32–34] has promoted the hole as a very good candidate as carrier of quantum bit information. There are also a few appealing theoretical proposals how the HH spin state can be manipulated [35–39].

In this Letter, we demonstrate by using a four-band HH-LH model that the motion of the valence hole in gated semiconductor nanostructures can induce the rotation of the HH spin in the presence of the Dresselhaus spin-orbit interaction (DSOI). Supported by these results we present an efficient scheme which can be used to realize any rotation of the HH spin and propose a nanodevice which acts as a quantum logic NOT gate on a HH spin qubit. The spin rotations are realized by transporting the hole along a closed loop which is defined by metal gates. This method is more suitable for controlling the hole spin than the application of a magnetic field, because the in-plane hole g factor is very small. Therefore, one would need a magnetic field of several Teslas, which is still experimentally challenging. Application of the multiband model allows us to study mixing between HH and LH states. We found that

in the considered nanostructures the HH-LH mixing is negligible so we can expect long coherence times for a qubit stored in the HH spin state [29–31].

We consider a planar heterostructure covered by nanostructured metal gates. The system consist of a 10-nm thick (unstrained) zinc-blende quantum well structure sandwiched between two 10-nm blocking barriers (Fig. 1) in which the single valence hole is confined. The hole which forms a charge distribution in this quantum well induces a response potential of the electron gas in the metallic gate which in turns leads to a self-focusing mechanism of the confined charged particle wave function [40]. Thus interaction of the hole with the metal is a source of additional lateral confinement. As a result the hole is self-trapped under the metal in the form of a stable Gaussian like wave packet. It has the unique property for a quantum particle, that it reflects from a barrier or tunnels through it with 100% probability while conserving its shape, which is rather a characteristic of classical objects. This property can be used to transfer a charged particle in the form of a stable wave packet (soliton) between different locations within the nanodevice by applying static weak voltages to the electrodes only [41]. We use a system of coordinates in which the quantum well is oriented in the $z[001]$ (growth) direction and the hole can move only in the $x[100] - y[010]$ plane. We consider the two dimensional four-band HH ($J_z = \pm 3/2$), LH ($J_z = \pm 1/2$) Hamiltonian:

$$\hat{H} = \hat{H}_{\mathrm{LK}} - |e|\phi(x, y, z_0)\hat{I} + \hat{H}^{\mathrm{2D}}_{\mathrm{BIA}}. \tag{1}$$

The first term is the Luttinger-Kohn Hamiltonian [42] describing the kinetic energy of the 2D hole, which for unstrained zinc blende materials can be written in the effective mass approximation as

$$\hat{H}_{\mathrm{LK}} = \begin{pmatrix} \hat{P}_+ & 0 & \hat{R} & 0 \\ 0 & \hat{P}_- & 0 & \hat{R} \\ \hat{R}^\dagger & 0 & \hat{P}_- & 0 \\ 0 & \hat{R}^\dagger & 0 & \hat{P}_+ \end{pmatrix}, \tag{2}$$

where $\hat{P}_\pm = \frac{\hbar^2}{2m_0}(\gamma_1 \pm \gamma_2)(k_x^2 + k_y^2) + E_0^\pm$ and $\hat{R} = \frac{\hbar^2}{2m_0}\sqrt{3}[\gamma_2(k_x^2 - k_y^2) - 2i\gamma_3 k_x k_y]$. We denote $E_0^\pm = \frac{\hbar^2}{2m_0}(\gamma_1 \mp 2\gamma_2)\langle k_z^2\rangle$ as the first subband energy in the z direction ($E_0^- = E_\perp^{\mathrm{LH}}$, $E_0^+ = E_\perp^{\mathrm{HH}}$) with $\langle k_z^2\rangle = \pi^2/d^2$, where d is the quantum well height, γ_1, γ_2, γ_3 are the Luttinger parameters and m_0 is the free electron mass. Momentum operators are $k_q = -i\frac{\partial}{\partial q}$ where $q = x, y$. We use the representation where the projections of Bloch angular momentum on the z axis are arranged in the following order $J_z = \frac{3}{2}, \frac{1}{2}, -\frac{1}{2}, -\frac{3}{2}$. Consistently with this convention, the state vector can be written as

$$\Psi(x, y, t) = (\psi^\uparrow_{\mathrm{HH}}(x, y, t), \psi^\uparrow_{\mathrm{LH}}(x, y, t), \psi^\downarrow_{\mathrm{LH}}(x, y, t), \psi^\downarrow_{\mathrm{HH}}(x, y, t))^{\mathbf{T}}. \tag{3}$$

The electrostatic potential $\phi(x, y, z_0, t)$, which is "felt" by the hole, is the source of the self-trapping potential. Its origin is due to charges induced on the metal electrodes. The potential is found by solving the Poisson equation in a three dimensional computational box containing the entire nanodevice. The detailed method was described in Refs. [17,41]. Quantum calculations [43] indicate that this is a good approximation of the actual response potential of the electron gas. The $\hat{I}$ is the unit operator, e is the elementary charge and z_0 is the center of the quantum well. The $\hat{H}_{\mathrm{BIA}}$ term accounts for the DSOI [44] which is caused by the lack of inversion symmetry of the crystal—a characteristic feature for zinc blende materials—and (including two main contributions) takes the following form for bulk [45]

$$\hat{H}_{\mathrm{BIA}} = -\beta_0 \boldsymbol{k} \cdot \boldsymbol{\Omega}_{\boldsymbol{J}} - \beta \boldsymbol{\Omega}_{\boldsymbol{k}} \cdot \boldsymbol{J}, \tag{4}$$

where $\boldsymbol{k} = (k_x, k_y, k_z)$ is the momentum vector and $\boldsymbol{J} = (J_x, J_y, J_z)$ is the vector of the 4×4 spin 3/2 matrices. The x component of $\boldsymbol{\Omega}_{\boldsymbol{O}}$ is the $\Omega^x_O = \{O_x, O_y^2 - O_z^2\}$ and Ω^y_O, Ω^z_O can be obtained by cyclic permutations, $\{A, B\} = \frac{1}{2}(AB + BA)$ and the operator $O = k, J$. Going from bulk to 2D systems and neglecting qubic k terms [46], the bulk DSOI can be directly transformed into

$$\hat{H}^{\mathrm{2D}}_{\mathrm{BIA}} = -\beta_0(k_x\Omega^x_J + k_y\Omega^y_J) + \beta\langle k_z^2\rangle(k_x J_x - k_y J_y), \tag{5}$$

where β_0 and β can be found in Refs. [45,47]. The time evolution of the system is described by the time-dependent Schrödinger equation which is solved numerically self-consistently with the Poisson equation. Due to the motion of the hole wave packet, the Poisson equation has to be solved in every time step of the iteration procedure. The initial condition is the ground state of the hole confined under the metal due to the self-focusing effect and is calculated by solving the stationary Schrödinger equation $\hat{H}\Psi_0(x, y) = E\Psi_0(x, y)$.

Let us consider the heterostructure from Fig. 1: an unstrained GaAs quantum well of 10-nm height sandwiched between two blocking barriers of 10-nm height, covered by a 65×65 nm square electrode (called e_1) and an approximately 4000-nm long electrode (called e_2), as also depicted in Figs. 2(d) and 2(d′). The distance between both electrodes is chosen to be 10 nm. This distance should be small enough so that when the hole wave function is located under electrode e_1, there is a small overlap with the area under electrode e_2. In the initial state, the hole is confined in the ground state under e_1, which can be

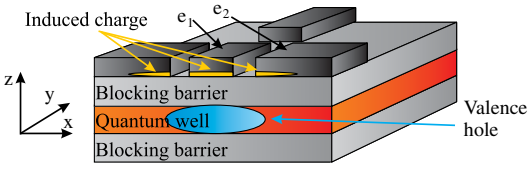

FIG. 1 (color online). Cross section of the nanodevice.

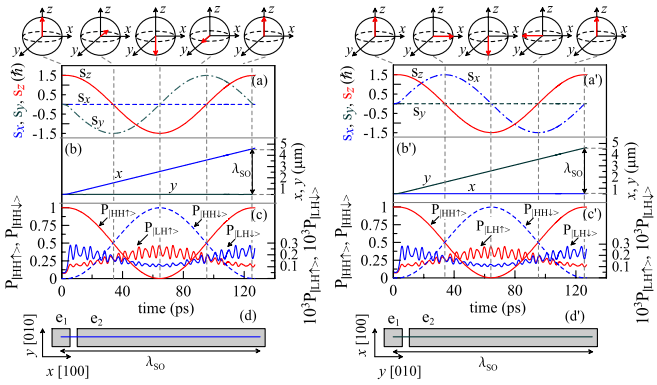

FIG. 2 (color online). Time evolution of the HH spin components (a), average position of the hole wave packet (b), and probability of occupying the following hole basis states (c): $|\mathrm{HH}\uparrow\rangle$, $|\mathrm{HH}\downarrow\rangle$, $|\mathrm{LH}\uparrow\rangle$, $|\mathrm{LH}\downarrow\rangle$, for a hole moving along the wire covered by the electrodes e_1, e_2 form figure (d). In (c) left (right) axis corresponds to probability of finding the hole in the HH (LH) spin states. Results for hole moving along the wire placed in $y\,(d')$ direction are depicted in (a′), (b′), and (c′). Above each plot, there are Bloch spheres representing the qubit after each $\pi/2$ rotation.

achieved by applying a voltage $V_1 = -0.3$ mV and $V_2 = 0$ to the electrodes e_1 and e_2, respectively [48]. We assume that the hole is in the initial state $\Psi(x, y, t_0) = (\psi^{\uparrow}_{\mathrm{HH}}(x, y, t_0), 0, 0, 0)^T$ [49]. The preparation of such a spin state—as well as its read-out—can be achieved without the application of a magnetic field by using the experimentally demonstrated high fidelity (99%) optical methods [25] or by using an analogous device, as proposed theoretically in Ref. [18], which acts on the HH spin. The hole is forced to move along the path under the electrode e_2 by changing the voltage configuration to $V_1 = 0$, $V_2 = -0.7$ mV. We plot the probability of finding the hole in the possible basis states $P_{J_z}(t) = \int |\psi_{J_z}(x, y, t)|^2 dxdy$ in Figs. 2(c) and 2(c′) where $J_z = 3/2, 1/2, -1/2, -3/2$. We observe that during the motion as well as in the ground state, the probability of finding the hole in the LH state is very small ($\sim 10^{-4}$). It shows that the mixing between HH and LH states is negligible in our system. By decreasing the quantum well height further, the HH-LH spliting energy $\Delta_{\mathrm{HL}} = E^{\mathrm{LH}}_{\perp} - E^{\mathrm{HH}}_{\perp}$ would increase and the probability of finding the system in the LH state would be reduced further.

Because of the fact that the hole is mainly composed of the HH state in the considered nanostuctures, we can calculate expectation values of the HH pseudospin 1/2 operator $\vec{s} = \langle \frac{3}{2}\vec{\sigma}\rangle_{\Psi_{\mathrm{HH}}}$ for the HH state defined as $\Psi_{\mathrm{HH}}(x, y, t) = (\psi^{\uparrow}_{\mathrm{HH}}(x, y, t), \psi^{\downarrow}_{\mathrm{HH}}(x, y, t))^T$ where $\vec{\sigma}$ are the Pauli spin 1/2 matrices. For a hole occupying only the HH band, the expectation values of total angular momentum $J = 3/2$ matrices are $\langle J_x\rangle = \langle J_y\rangle = 0$ and $\langle J_z\rangle = s_z$. The time dependence of the HH average spin components are given in Figs. 2(a) and 2(a′). During the motion of a hole along the x (y) axis, the s_x (s_y) spin component is preserved and s_y (s_x), s_z components oscillate: the HH spin is rotated around the axis parallel to the direction of motion. This behavior can be understood by analyzing an approximated $\hat{H}_{\mathrm{BIA}}$ Hamiltonian for the HH band only [50]

$$\hat{H}^{\mathrm{HH}}_{\mathrm{BIA}} = -\frac{\tilde{\beta}}{3}[(p_x^3 + p_x p_y^2)\sigma_x + (p_y^3 + p_x^2 p_y)\sigma_y]. \quad (6)$$

For quantum wires placed along the q direction, the above Hamiltonian can be approximated by $\hat{H}^{\mathrm{HH}}_{\mathrm{BIA},q} = -\frac{\tilde{\beta}}{3}(p_q^3 + p_q\langle p_{q_\perp}^2\rangle)\sigma_q$, where $q = x, y$, $q_\perp$ axis is perpendicular to q and the $\tilde{\beta}$ is an effective DSOI coupling strength given in [50]. From the fact that the momentum operators p_q and p_q^3 are multiplied by the HH spin operator σ_q, one can expect that the hole motion with p_q momentum will generate a spin rotation around the q axis according to the time evolution operator $\hat{U}_q(t) = e^{-i\hat{H}^{\mathrm{HH}}_{\mathrm{BIA},q}t/\hbar}$.

After traveling a certain distance $\lambda(t)$, the spin is rotated by the angle $\phi(t) = 2\pi\frac{\lambda(t)}{\lambda_{SO}}$. Thus, one can say that a unitary operation was performed on the HH spin state. One can derive the corresponding unitary spin rotation operator for a hole moving in the wire placed along the x axis:

$$\hat{R}_x(\phi) = \frac{1}{\sqrt{2}}\begin{pmatrix} i\sqrt{1+\cos(\phi)} & \frac{\sin(\phi)}{\sqrt{1+\cos(\phi)}} \\ \frac{\sin(\phi)}{\sqrt{1+\cos(\phi)}} & i\sqrt{1+\cos(\phi)} \end{pmatrix} \quad (7)$$

and for a hole moving in the wire which is placed along the y direction:

$$\hat{R}_y(\phi) = \frac{1}{\sqrt{2}}\begin{pmatrix} \sqrt{1+\cos(\phi)} & -\frac{\sin(\phi)}{\sqrt{1+\cos(\phi)}} \\ \frac{\sin(\phi)}{\sqrt{1+\cos(\phi)}} & \sqrt{1+\cos(\phi)} \end{pmatrix}. \quad (8)$$

The hole restores its initial spin after passing the distance λ_{SO} which depends on the DSOI coupling strengths and the effective mass (Luttinger parameters). The presented results are obtained for a GaAs quantum well and taking into account the full DSOI Hamiltonian (5). We also performed calculations for other materials ZnSe, and CdTe and estimated the λ_{SO} length: $\lambda_{SO}^{\mathrm{GaAs}} \approx 4.05$ μm, $\lambda_{SO}^{\mathrm{ZnSe}} \approx 0.86$ μm, $\lambda_{SO}^{\mathrm{CdTe}} \approx 0.74$ μm [51]. It is worth mentioning that the "on-demand" single electron transport on such distances (μm), and even much larger, was recently realized experimentally using surface acoustic waves [52,53].

Taking advantage of the fact that the hole motion generates HH spin rotations, one can design a gated semiconductor nanodevice that will act on the HH spin qubit as a quantum gate. We propose a nanodevice covered by the system of electrodes from Fig. 3(d) which act as a quantum NOT gate. The hole whose spin we want to transform is initially confined under the 65×65 nm electrode e_1, where a constant $V_1 = -0.2$ mV voltage is applied while the voltage on the other electrodes is set to zero. Electrodes are separated by a distance of 10 nm. Let us assume that the

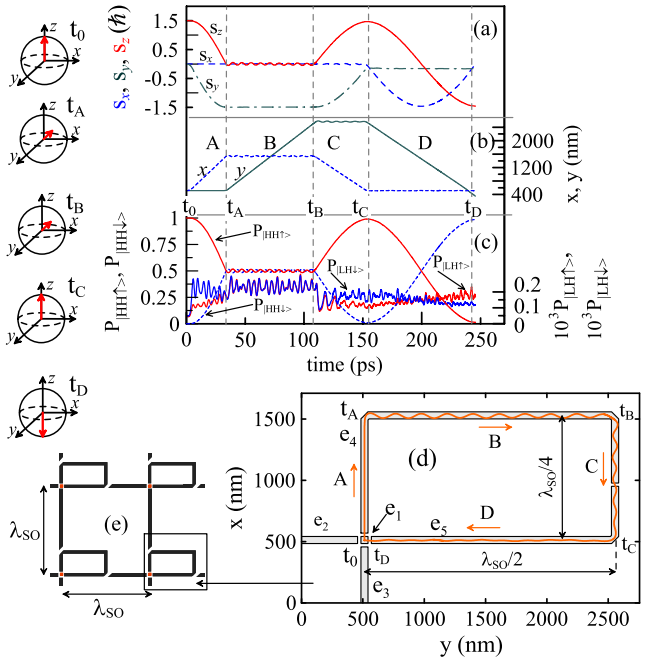

FIG. 3 (color online). (a),(b) and (c) same as Figs. 2(a)–2(c), but for the quantum NOT gate which is covered by the system of electrodes e_1-e_5 presented in (d). In (d) the solid orange line represents the hole trajectory (orange arrow represents direction of motion of the hole). Hole initially confined under e_1 goes to the $+x$ direction passing A, B, C, and D segments of the loop. Vector state is depicted on the Bloch spheres in the subsequent moments of time: $t_0 - t_D$. Scheme in figure (e) illustrates the scalability of the nanodevice. Spins of the different holes confined under the red electrodes form a quantum register, and on each qubit quantum logic gate can be separately applied by means of small electric fields.

hole is in the ground state with its initial spin state prepared to the HH spin up state. By changing the voltage applied to e_1 to $V_1 = 0$ and switching the voltage on e_4 to $V_4 = -0.7$ mV the hole starts to move in the $+x$ direction under electrode e_4. After passing a $\lambda_{SO}/4$ distance of segment A, the HH spin is rotated around the x axis by an angle $\pi/2$, and the $\hat{R}_x(\pi/2)$ operation is performed. At the end of segment A, the hole wave packet turns right and starts to move parallel to the y axis. During the reflection the hole wave packet does not scatter due to the self-focusing effect. The hole passes the B segment whose length is $\lambda_{SO}/2$ performing the $\hat{R}_y(\pi)$ operation and turns right. Then hole goes under electrode e_5 whose voltage was in the meantime set to the voltage of the e_4 electrode. The hole moves in $-x$ and $-y$ directions performing the $\hat{R}_x(-\pi/2)$ and $\hat{R}_y(-\pi)$ operation. Finally, the hole returns to its initial position under the e_1 electrode, where it is captured by applying the $V_1 = -1.0$ mV voltage. After passing the whole loop, a set of HH spin transformations is performed resulting in a NOT gate operation $\hat{U}_{\mathrm{NOT}} = \hat{R}_y(-\pi)\hat{R}_x(-\pi/2)\hat{R}_y(\pi)\hat{R}_x(\pi/2) = -i\sigma_x$. Since the hole after completing the set of transformations returns to its initial position, the gate operation is performed on the HH spin exclusively, not on the spatial part of the wave function. The size of the gate depends only on the λ_{SO} length for the considered material.

The gate operation time for GaAs and applied starting voltage configuration is $t_{\mathrm{NOT}}^{\mathrm{GaAs}} \approx 250$ ps. As the time is proportional to λ_{SO} the gate operation time for other materials is significantly improved reaching $t_{\mathrm{NOT}}^{\mathrm{CdTe}} \approx 60$ ps and $t_{\mathrm{NOT}}^{\mathrm{ZnSe}} \approx 80$ ps.

The dipolar hyperfine interaction could affect the fidelity of the proposed gate. But, as demonstrated, the HH/LH mixing can be neglected and the dipolar hyperfine interaction for pure HH spin states is of the Ising type [29,30], leading to a HH spin coherence time which was experimentally determined to be at least 100 ns [26]. Thus, the proposed gate can be applied about $\sim 10^3$ times until the HH spin coherence will be lost. Our proposal can also be extended to a larger number of qubits that can be integrated in a single nanodevice. This scalability is shown in Fig. 3(e). Furthermore, the proposed device is suitable for coherent transport of a hole wave packet and thus allows for transferring quantum information between different locations in this nanodevice.

In conclusion, we showed that the motion of the hole in gated semiconductor heterostructures can induce a coherent rotation of the HH spin where the DSOI is the mediator of this process. An important result is that during the motion in the presence of the DSOI, the mixing between HH and LH states is negligible from which we can expect that the proposed HH spin qubit should be robust to decoherence coming from the interaction with the nuclear spins. We proposed a quantum NOT gate which operates in subnanoseconds, and it is controlled only by means of small static local electric fields generated by the top gates. It allows us to address the HH spin qubit individually, making our proposal scalable.

This work was supported by the Grant No. N N202 128337 from the Ministry of Science and Higher Education, as well as by the "Krakow Interdisciplinary PhD-Project in Nanoscience and Advances Nanostructures" operated within the Foundation for Polish Science MPD Programme and cofinanced by European Regional Development Fund, the Belgian Science Policy (IAP), and the Flemish Science Foundation (FWO-V1).

[1] D. Awshalom, D. Loss, and N. Samarth, *Semiconductor Spintronics and Quantum Computation* (Springer Verlag, Berlin, 2002).
[2] I. Zutic, J. Fabian, and S. Das Sarma, Rev. Mod. Phys. **76**, 323 (2004).
[3] D. P. DiVincenzo, Fortschr. Phys. **48**, 771 (2000).
[4] D. Loss and D. P. DiVincenzo, Phys. Rev. A **57**, 120 (1998).
[5] R. Hanson, L. P. Kouwenhoven, J. R. Petta, S. Tarucha, and L. M. K. Vandersypen, Rev. Mod. Phys. **79**, 1217 (2007).

[6] S. Amasha, K. MacLean, I. P. Radu, D. M. Zumbühl, M. A. Kastner, M. P. Hanson, and A. C. Gossard, Phys. Rev. Lett. **100**, 046803 (2008).

[7] J. R. Petta, A. C. Johnson, J. M. Taylor, E. A. Laird, A. Yacoby, M. D. Lukin, C. M. Marcus, M. P. Hanson, and A. C. Gossard, Science **309**, 2180 (2005).

[8] J. M. Elzerman, R. Hanson, L. H. Willems van Beveren, B. Witkamp, L. M. K. Vandersypen, and L. P. Kouwenhoven, Nature (London) **430**, 431 (2004).

[9] T. Meunier, I. T. Vink, L. H. Willems van Beveren, F. H. L. Koppens, H. P. Tranitz, W. Wegscheider, L. P. Kouwenhoven, and L. M. K. Vandersypen, Phys. Rev. B **74**, 195303 (2006).

[10] F. H. L. Koppens, C. Buizert, K. J. Tielrooij, I. T. Vink, K. C. Nowack, T. Meunier, L. P. Kouwenhoven, and L. M. K. Vandersypen, Nature (London) **442**, 766 (2006).

[11] A. Morello, J. J. Pla, F. A. Zwanenburg, K. W. Chan, K. Y. Tan, H. Huebl, M. Möttönen, C. D. Nugroho, C. Yang, J. A. van Donkelaar, A. D. C. Alves, D. N. Jamieson, C. C. Escott, L. C. L. Hollenberg, R. G. Clark, and A. S. Dzurak, Nature (London) **467**, 687 (2010).

[12] K. C. Nowack, F. H. L. Koppens, Yu. V. Nazarov, and L. M. K. Vandersypen, Science **318**, 1430 (2007).

[13] S. Nadj-Perge, S. M. Frolov, E. P. A. M. Bakkers, and L. P. Kouwenhoven, Nature (London) **468**, 1084 (2010).

[14] V. N. Golovach, M. Borhani, and D. Loss, Phys. Rev. B **74**, 165319 (2006).

[15] S. Debald and C. Emary, Phys. Rev. Lett. **94**, 226803 (2005).

[16] C. Flindt, A. S. Sorensen, and K. Flensberg, Phys. Rev. Lett. **97**, 240501 (2006).

[17] S. Bednarek and B. Szafran, Phys. Rev. Lett. **101**, 216805 (2008).

[18] S. Bednarek, P. Szumniak, and B. Szafran, Phys. Rev. B **82**, 235319 (2010).

[19] I. A. Merkulov, Al. L. Efros, and M. Rosen, Phys. Rev. B **65**, 205309 (2002).

[20] A. V. Khaetskii, D. Loss, and L. Glazman, Phys. Rev. Lett. **88**, 186802 (2002).

[21] J. Fischer and D. Loss, Science **324**, 1277 (2009).

[22] G. Burkard, Nature Mater. **7**, 100 (2008).

[23] M. H. Kolodrubetz and J. R. Petta, Science **325**, 42 (2009).

[24] D. Heiss, S. Schaeck, H. Huebl, M. Bichler, G. Abstreiter, J. J. Finley, D. V. Bulaev, and D. Loss, Phys. Rev. B **76**, 241306 (2007).

[25] B. D. Gerardot, D. Brunner, P. A. Dalgarno, P. Öhberg, S. Seidl, M. Kroner, K. Karrai, N. G. Stoltz, P. M. Petroff, and R. J. Warburton, Nature (London) **451**, 441 (2008).

[26] D. Brunner, B. D. Gerardot, P. A. Dalgarno, G. Wüst, K. Karrai, N. G. Stoltz, P. M. Petroff, and R. J. Warburton, Science **325**, 70 (2009).

[27] F. Fras, B. Eble, P. Desfonds, F. Bernardot, C. Testelin, M. Chamarro, A. Miard, and A. Lemaître, Phys. Rev. B **84**, 125431 (2011).

[28] B. Eble, C. Testelin, P. Desfonds, F. Bernardot, A. Balocchi, T. Amand, A. Miard, A. Lemaître, X. Marie, and M. Chamarro, Phys. Rev. Lett. **102**, 146601 (2009).

[29] C. Testelin, F. Bernardot, B. Eble, and M. Chamarro, Phys. Rev. B **79**, 195440 (2009).

[30] J. Fischer, W. A. Coish, D. V. Bulaev, and D. Loss, Phys. Rev. B **78**, 155329 (2008).

[31] E. A. Chekhovich, A. B. Krysa, M. S. Skolnick, and A. I. Tartakovskii, Phys. Rev. Lett. **106**, 027402 (2011).

[32] K. De Greve, P. L. McMahon, D. Press, T. D. Ladd, D. Bisping, C. Schneider, M. Kamp, L. Worschech, S. Höfling, A. Forchel, and Y. Yamamoto, Nature Phys. **7**, 872 (2011).

[33] A. Greilich, S. G. Carter, D. Kim, A. S. Bracker, and D. Gammon, Nature Photon. **5**, 702 (2011).

[34] T. M. Godden, J. H. Quilter, A. J. Ramsay, Yanwen Wu, P. Brereton, S. J. Boyle, I. J. Luxmoore, J. Puebla-Nunez, A. M. Fox, and M. S. Skolnick, Phys. Rev. Lett. **108**, 017402 (2012).

[35] D. V. Bulaev and D. Loss, Phys. Rev. Lett. **98**, 097202 (2007).

[36] C. Y. Hsieh, R. Cheriton, M. Korkusinski, and P. Hawrylak, Phys. Rev. B **80**, 235320 (2009).

[37] J. C. Budich, D. G. Rothe, E. M. Hankiewicz, and B. Trauzettel, Phys. Rev. B **85**, 205425 (2012).

[38] T. Andlauer and P. Vogl, Phys. Rev. B **79**, 045307 (2009).

[39] R. Roloff, T. Eissfeller, P. Vogl, and W. Pötz, New J. Phys. **12**, 093012 (2010).

[40] S. Bednarek, B. Szafran, and K. Lis, Phys. Rev. B **72**, 075319 (2005).

[41] S. Bednarek, B. Szafran, R. J. Dudek, and K. Lis, Phys. Rev. Lett. **100**, 126805 (2008).

[42] J. M. Luttinger and W. Kohn, Phys. Rev. **97**, 869 (1955).

[43] S. Bednarek and B. Szafran, Phys. Rev. B **73**, 155318 (2006).

[44] G. Dresselhaus, Phys. Rev. **100**, 580 (1955).

[45] R. Winkler, *Spin-Orbit Coupling Effects in Two Dimensional Electron and Hole Systems* (Springer, Berlin, 2003).

[46] We can neglect the cubic Dresselhaus term since in the proposed device the lateral size ($l \approx 65$ nm) of the induced quantum dot is larger than the quantum well height ($d = 10$ nm). Therefore, the cubic Dresselhaus term is smaller than the linear one by a factor of $(d/l)^2$, which is of the order of ~ 0.01.

[47] M. Cardona, N. E. Christensen, and G. Fasol, Phys. Rev. B **38**, 1806 (1988).

[48] Since the metal gate is in contact with an undoped semiconductor, the Schottky barrier V_B should be taken into account with mV accuracy. Therefore, the potential applied to the gates is equal to $V_i \rightarrow V_i - V_B$.$V_B$ should be determined experimentally for a certain structure.

[49] In fact due to lateral confinement ground state of the hole in induced quantum dot has some small amount ($< 0.1\%$) of LH states Fig. 2(c).

[50] D. V. Bulaev and D. Loss, Phys. Rev. Lett. **95**, 076805 (2005).

[51] We use Luttinger parameters (γ_1, γ_2, γ_3) and delectric constant (ϵ): $\gamma_1^{\mathrm{GaAs}} = 6.85$, $\gamma_2^{\mathrm{GaAs}} = 2.1$, $\gamma_3^{\mathrm{GaAs}} = 2.9$, $\epsilon^{\mathrm{GaAs}} = 12.4$, $\gamma_1^{\mathrm{CdTe}} = 5.3$, $\gamma_2^{\mathrm{CdTe}} = 1.7$, $\gamma_3^{\mathrm{CdTe}} = 2.$, $\epsilon^{\mathrm{CdTe}} = 10.125$, $\gamma_1^{\mathrm{ZnSe}} = 4.3$, $\gamma_2^{\mathrm{ZnSe}} = 1.14$, $\gamma_3^{\mathrm{ZnSe}} = 1.84$, $\epsilon^{\mathrm{ZnSe}} = 9.14$ taken from Table D.1 from Ref. [45].

[52] S. Hermelin, S. Takada, M. Yamamoto, S. Tarucha, A. D. Wieck, L. Saminadayar, C. Bäuerle, and T. Meunier, Nature (London) **477**, 435 (2011).

[53] R. P. G. McNeil, M. Kataoka, C. J. B. Ford, C. H. W. Barnes, D. Anderson, G. A. C. Jones, I. Farrer, and D. A. Ritchie, Nature (London) **477**, 439 (2011).